SGP-TR-145-33

PROCEEDINGS

EIGHTEENTH WORKSHOP
GEOTHERMAL RESERVOIR ENGINEERING

January 26-28, 1993

Henry J. Ramey, Jr., Roland N. Horne,
Paul Kruger, Frank G. Miller,
William E. Brigham, Jean W. Cook
Stanford Geothermal Program
Workshop Report SGP-TR-145

DISCLAIMER

PROCEEDINGS, Eighteenth Workshop on Geothermal Reservoir Engineering
Stanford University, Stanford, California, January 26-28, 1993
SGP-TR-145

AN EVALUATION OF THE DEEP RESERVOIR CONDITIONS OF THE BACON-MANITO GEOTHERMAL FIELD, PHILIPPINES USING WELL GAS CHEMISTRY

by Franco D'Amore*, Marinela Maniquis-Buenviaje Φ and Ramonito P. Solis Φ

* CNR-IIRG, 2 Piazza Solferino, 56126 Pisa, Italy
Φ PNOC-EDC, Ft. Bonifacio, Metro Manila, Philippines

ABSTRACT

Gas chemistry from 28 wells complement water chemistry and physical data in developing a reservoir model for the Bacon-Manito geothermal project (BMGP), Philippines. Reservoir temperature, T_{HSH}, and steam fraction, *y*, are calculated or extrapolated from the grid defined by the Fischer-Tropsch (FT) and H_2-H_2S (HSH) gas equilibria reactions. A correction is made for H_2 that is lost due to preferential partitioning into the vapor phase and the reequilibration of H_2S after steam loss.

INTRODUCTION

The Bacon-Manito geothermal project (BMGP) is located 20 kms southeast of Legazpi City, in the northern Philippine island of Luzon (Fig. 1). Initial geoscientific surveys were conducted in 1977 and exploratory drilling followed in 1978. At present, over 30 wells have been drilled. The 110-MWe BacMan I and 2 x 20 MWe BacMan II geothermal power plants are presently being built and are scheduled for commissioning in 1993.

Fault structures is the major cause of permeability at BMGP (PNOC-EDC, 1988). Based on subsurface geology, permeability is mostly due to the intersection of faults mapped on the surface and faults accompanied by dike intrusions.

The main components of the lithologic unit in BMGP are the Gayong Sedimentary Formation (GSF), Pocdol Volcanics (PV), and Cawayan Intrusive Complex (CIC). The GSF is composed primarily of calcareous sedimentary breccias. The lower PV is composed of hyaloclastites, andesites and basalts; while the upper PV is composed of fresh hornblende-bearing andesite, intensely to completely altered volcanic rock

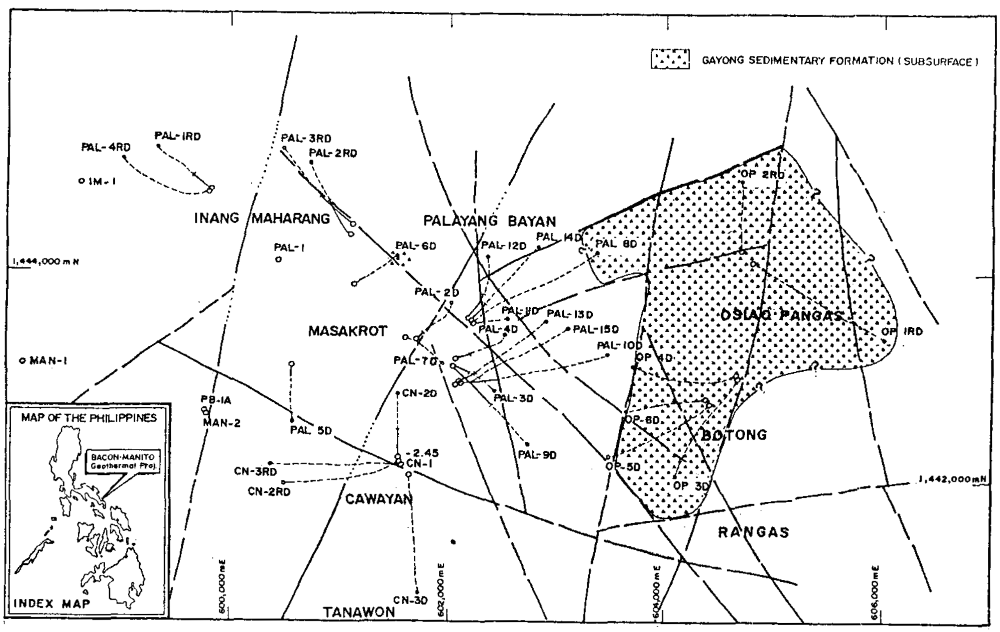

Fig. 1 Location Map of BMGP

intercalated with andesitic breccias, lavas and tuffs. The CIC include all basalt/diabase, microdiorite and plutonic dikes that intrude the GSF and PV.

BACMAN RESERVOIR CHEMISTRY

Except for three wells, Pal-2D, CN-2D and CN-2RD, all of the wells in BMGP discharge near neutral NaCl waters. Several wells, located in Cawayan and Palayang Bayan sectors, encounter cool meteoric or acidic SO_4-rich condensate type fluids at shallower depths.

Geochemical field trends, represented here by reservoir chloride field trend, suggest that the whole BMGP area belong to one geothermal system (Fig. 2). The center of the resource is inferred to be close to wells OP-3D, OP-4D, Pal-8D, Pal-10D and Pal-14D. The deep reservoir chloride of about 6500 mg/kg is almost uniform across the central Palayang Bayan area. The upflowing fluid has a reservoir chloride close to 8000 mg/kg.

The baseline or pre-exploitation steam chemistry of BMGP wells are presented in Table 1. These data are taken when the well is producing from the major feedzone at stabilized conditions during discharge testing. CO_2 comprises 95-98% by volume of the non-condensible gas in the steam phase. The rest is composed of N_2, CH_4, Ar, NH_3 and H_2.

Wells in Palayang Bayan and Cawayan with high gas concentrations produce predominantly from a shallow level, leading early workers to infer the presence of a shallow gassy, two-phase region or a gas cap (PNOC-EDC, 1988; KRTA, 1986).

DATA PROCESSING

Theoretical Background

The following expressions can be used together to calculate the reservoir temperature, T_{HSH} and steam fraction, y:

$$4\log(H_2/H_2O)_d - \log(CH_4/CO_2)_d = FT_d \qquad \text{Eq. (1)}$$

$$3\log(H_2S/H_2O)_d - \log(H_2/H_2O)_d = HSH_d \qquad \text{Eq. (2)}$$

where $(i/H_2O)_d$ is the molar ratio at the disharge point "d".

When $y \geq 0$, the graphical solution is used. The method used by D'Amore and Truesdell (1985) implies isothermal conditions during steam loss. The reservoir temperature for these wells are equal to the temperature at which the fluid boils upon ascent.

In some cases extremely negative values of y are extrapolated and steam loss is not consistent with the local conditions of the reservoir liquid as seen in Southern Negros geothermal project, Philippines (D'Amore et al, in preparation), so that:

$$FT_d = -15.35 - 3952.8/T^\circ + 4.635\log T^\circ - 4\log B^\circ_{H_2} - \log B^\circ_{CO_2} + \log B^\circ_{CH_4} - 4\log(1+y-yB_{H_2}) - \log(1+y-yB_{CO_2}) + \log(1+y-yB_{CH_4}) \qquad \text{Eq. (3)}$$

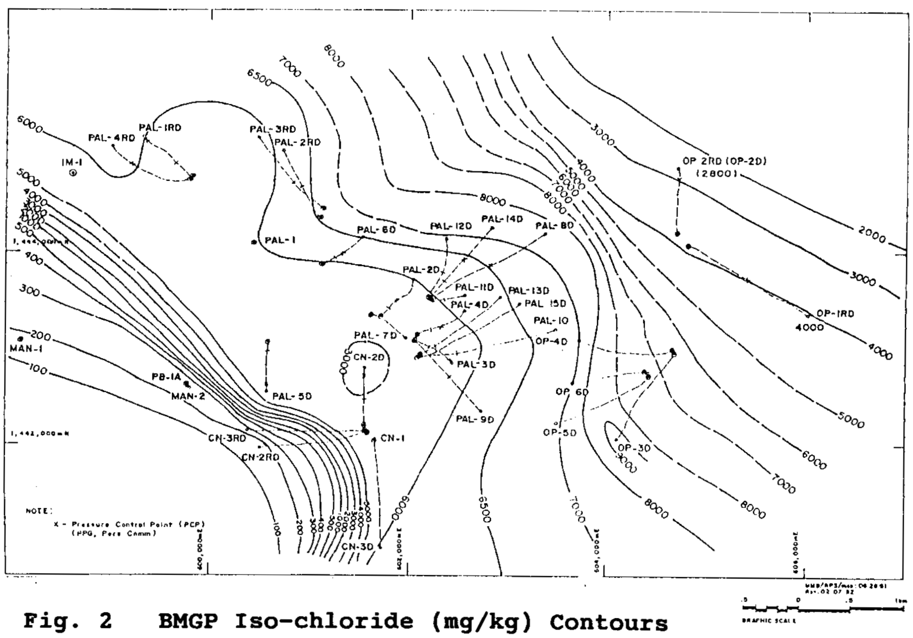

Fig. 2 BMGP Iso-chloride (mg/kg) Contours

TABLE 1: BACON-MANITO BASELINE WELL STEAM CHEMISTRY

WELL	DATE mm-dd-yy	WHP MPaa	H kJ/kg	SP MPaa	pH	CO2	H2S	N2	H2	CH4
						mmoles/100 moles H2O at TD				
PAL-1	01-01-83	1.18	1077	0.640	6.87	146	0.90	1.513	0.052	1.660
PAL-2D	03-12-84	2.75	1281	0.611	5.33	1471	13.80	13.27	0.721	10.765
PAL-3D	05-20-83	2.51	1255	0.570	6.38	169	5.55	0.224	0.017	0.163
PAL-4D	12-20-83	3.35	1308	0.349	7.51	321	6.98	0.236	0.108	4.280
PAL-5D	07-12-84	1.82	1230	0.542	7.49	34	0.99	1.070	0.019	0.400
PAL-6D	06-07-84	0.31	1547	0.225	7.01	398	3.29	1.760	0.242	3.047
PAL-7D	08-07-84	1.58	1162	0.832	6.38	218	1.99	1.264	0.086	3.234
PAL-8D	04-12-84	4.44	1479	0.619	7.16	772	9.60	0.374	0.095	1.452
PAL-9D	11-26-86	2.39	1158	0.429	7.68	105	3.98	0.310	0.050	0.800
PAL-10D	12-19-85	1.62	1407	0.904	6.66	620	13.70	0.461	0.863	7.387
PAL-11D	10-31-87	1.09	1526	0.814	6.90	870	11.30	2.090	0.390	11.550
PAL-12D	05-06-88	3.27	1353	0.839	7.03	327	5.76	0.953	0.054	2.914
PAL-13D	03-08-87	3.54	1277	0.910	6.84	264	7.00	0.390	0.203	1.213
PAL-13D	03-17-87	0.88	1345	0.625	6.83	339	7.58	2.530	0.765	5.170
PAL-14D	01-13-89	1.37	1334	0.551	7.15	255	4.39	1.200	0.035	1.703
PAL-15D	12-14-89	2.54	1218	0.504	6.50	196	6.30	0.682	0.044	0.403
PAL-1RD	09-28-84	1.33	1099	0.702	7.41	65	0.85	0.372	0.014	0.409
PAL-3RD	02-04-85	0.32	1280	0.262	7.49	260	1.90	1.490	0.091	6.060
OP-1RD	07-20-88	0.37	1256	0.130	7.95	1409	9.20	0.960	0.220	43.900
OP-2RD	08-18-88	0.48	848	0.391	8.06	613	1.76	0.110	0.025	5.048
OP-3D	01-22-90	1.53	1581	0.413	7.53	1286	31.10	2.060	6.780	35.900
OP-4D	07-16-91	5.65	1478	0.473	6.46	833	18.50	0.570	1.430	3.350
OP-5D	09-21-91	0.27	2457	0.227	6.49	1796	40.10	3.410	7.950	30.200
OP-6D	03-16-91	0.96	2526	0.606	7.74	3592	100.00	4.890	27.03	92.460
CN-1	11-19-82	2.37	1214	0.5/7	7.71	50	1.85	0.063	0.027	0.917
CN-2D	10-07-82	0.68	1331	0.649	3.79	4381	16.07	5.613	3.557	132.56
CN-3D	10-20-90	2.20	1297	0.825	7.25	70	3.30	0.710	0.090	0.980
CN-2RD	05-10-91	0.51	965	0.433	3.66	68	2.60	4.900	0.560	0.910
CN-3RD	09-13-91	0.35	922	0.333	8.57	80	0.45	7.600	0.218	0.864

$$HSH_d = 6.449 - 6149.7/T^{\circ} - 0.412\log T^{\circ} - 3\log B^{\circ}_{H_2S} + \log B^{\circ}_{H_2} - 3\log(1+y-yB_{H_2S}) + \log(1+y-yB_{H_2}) \quad \text{Eq. (4)}$$

where T° = reservoir temperature
B° = gas distribution coefficient at T°
B = gas distibution coefficient at temperature of steam loss
y = reservoir steam fraction

Application

Initially, T_{HSH} and y for these wells were taken from the isotherms in the grid defined by the FT-HSH equilibria at $y \geq 0$. About half of the wells were found to have y values ranging from -0.5% to +5% (Fig. 3). The rest of the wells, however, have highly negative y values.

For the latter wells, HSH_d at $y = 0$ was used to calculate T_{HSH} using Eq. (4). This is taken to be the local tempera-

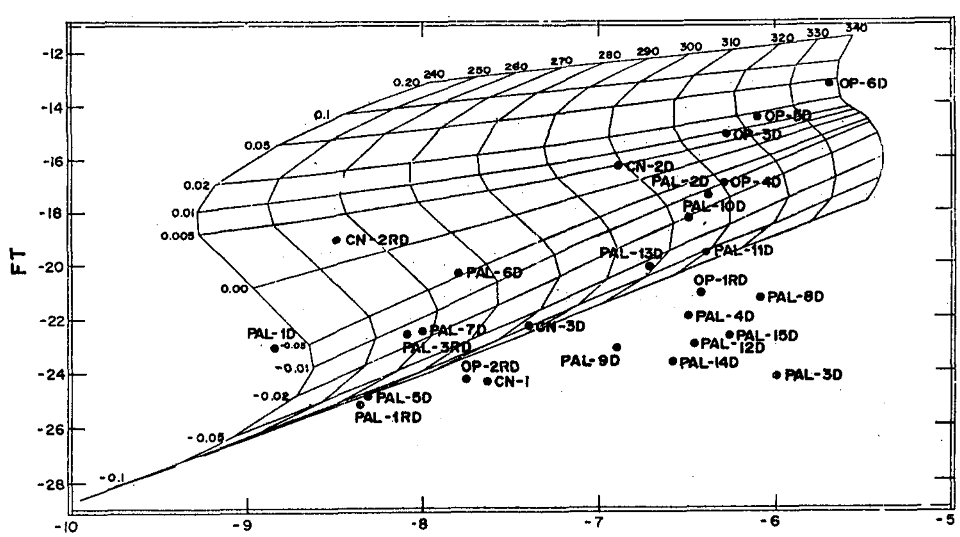

Fig. 3 FT-HSH Plot of BMGP Wells

ture of the aquifer after steam loss, hypothesizing reequilibration of H_2S. Assuming $T° = T_{HSH}$, y is calculated from Eq. (3) using an arbitrary degassing temperature of 240°C.

The use of 240°C as degassing temperature, however, can be justified using the two available analyses for well Pal-13D. At higher wellhead pressure (WHP), a decline in all components, especially in the less soluble H_2, CH_4 and N_2 is seen. In particular, H_2 decreases by about 75% while H_2S decline is small. The FT-HSH grid can be used for the Pal-13D gas data at low WHP. Extrapolation yields a temperature close to 285°C and y value close to zero. This temperature is very close to that measured at depth and also that using quartz geothermometer (Table 2). Assuming 290°C for the undisturbed system and using the first set of gas data at higher WHP in Eqs. (3) and (4), the degassing temperature and y are estimated. Convergency is obtained only at a degassing temperature of 240°C and y = -0.01.

Therefore, a degassing temperature of 240°C is assumed near the vicinity of Pal-13D. Much of the steam loss occurs close to a permeability barrier or shift from limestone sediments to more permeable volcanics, in between wells OP-4D/Pal-10D and Pal-15D, OP-5D and Pal-9D, Pal-8D and Pal-14D. As the hot geothermal fluids flows to the west, this value decreases to about 200°C. If 200°C degassing temperature is assumed, the computed y values will be less negative and probably close to zero.

DISCUSSION

Comparison with Other Reservoir Temperature Values

Fair correlation exists between T_{HSH}, T_{SiO2} (Fournier and Potter, 1982) and measured downhole temperatures (Fig. 4). Temperature differences up to 50°C may be due to the following reasons:

a) discharge enthalpy is greater than 1800 kj/kg and have steam-dominated discharge (OP-5D and OP-6D);

b) excess enthalpy (OP-3D, Pal-2D, Pal-10D, Pal-11D and Pal-15D);

c) the production zone is tapping a cooler reservoir fluid (CN-2RD and Pal-3RD); and

d) high CO_2 content depresses downhole temperatures

TABLE 2 : BMGP RESERVOIR TEMPERATURE AND STEAM FRACTION

WELL	DATE mm-dd-yy	STM.FR. y	RESERVOIR TEMPERATURE ESTIMATES TSiO2	Tmax	Tmajor	THSH
PAL-1	01-01-83	-0.004	243	281	240	236
PAL-2D	03-12-84	-0.012	280	293	267	305
PAL-3D	05-20-83	-0.150	270	285	278	308
PAL-4D	12-20-83	-0.027	276	307	286	300
PAL-5D	07-12-84	-0.033	260	270	-	250
PAL-6D	06-07-84	-0.005	273	286	279	266
PAL-7D	08-07-84	-0.015	272	277	277	263
PAL-8D	04-12-84	-0.038	291	313	313	310
PAL-9D	11-26-86	-0.050	275	282	282	288
PAL-10D	12-19-85	-0.004	283	325	283	305
PAL-11D	10-31-87	-0.012	280	270	270	305
PAL-12D	05-06-88	-0.075	282	299	299	300
PAL-13D	03-08-87	-	288	316	283	295
PAL-14D	01-13-89	-0.100	299	301	285	297
PAL-15D	12-14-89	-0.080	285	285	267	306
PAL-1RD	09-28-84	-0.038	245	260	256	250
PAL-3RD	02-04-85	-0.010	235	271	225	260
OP-1RD	07-20-88	-	253	245	230	305
OP-2RD	08-18-88	-0.035	209	216	186	265
OP-3D	01-22-90	0.010	296	300	294	317
OP-4D	07-16-91	-0.001	317	>300	313	313
OP-5D	09-21-91	0.020	279	296	270	323
OP-6D	03-16-91	0.050	290	>300	276	338
CN-1	11-19-82	-0.052	266	271	266	268
CN-2D	10-07-82	0.005	241	246	-	299
CN-3D	10-20-90	-0.018	274	276	272	275
CN-2RD	05-10-91	0.002	247	245	234	256
CN-3RD	09-13-91	0.003	233	239	234	213

TSiO2 = silica temperature (Fournier and Potter, 1982)
Tmax = measured maximum downhole temperature
Tmajor = measured temperature at major production zone
THSH = reservoir temperature based on gas chemistry, assuming FT-HSH equilibria

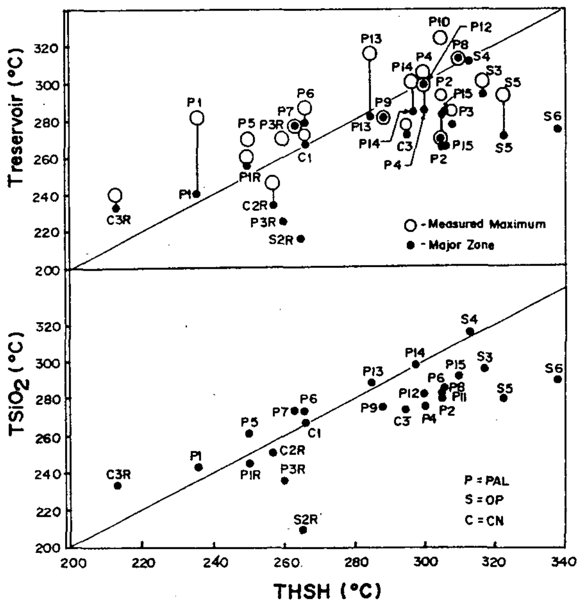

Fig. 4 Comparison of THSH with $TSiO_2$ and Measured Downhole Temperatures

The presence of gas has an effect on the pressure-temperature relationship and depresses the boiling point. The maximum temperature depression is 50°C at OP-2RD (36% by weight of steam). For other gassy wells like Pal-2D, Pal-8D, Pal-10D and Pal-11D, temperature decrease from 10 to 15°C. More specifically, the presence of a gassy, upper feedzone does not significantly affect the pressure profile but affects flow temperature below the gas feedzone (Aunzo, 1990).

e) measured temperatures are that of the steam and not the rock-water system for Botong wells OP-3D, OP-5D and OP-6D

In vapor-dominated systems, lower temperature steam is generated from boiling.

Field Trends

The results of T_{HSH} and y, are plotted across the field and temperature contours are drawn (Fig. 5). The main heat upflow zone as delineated by the tentative 320° contour is near the Botong sector. Reservoir temperature decreases towards the general westward direction. Reservoir steam fraction values, y (enclosed in parenthesis in Fig. 5), show a large variation across the field. Wells located near the heat upflow zone have y > 0%.

Reservoir Model

The above field trends also suggest that the whole BMGP area belongs to one geothermal system. Slightly two-phase (maximum y = 5%) reservoir fluids of temperature ≥ 320°C undergo adiabatic cooling and non-isothermal boiling along a postulated permeability barrier located near wells OP-4D, OP-5D, Pal-8D, Pal-9D, Pal-10D, Pal-13D, Pal-14D and Pal-15D (Fig. 6). The upflow zone is probably located near the vicinity of OP-3D to 6D.

The more mobile vapor phase flows through the shallow layers of the volcanics formation and outflows to the W-NW. This vapor-rich layer is both adiabatically and conductively cooled as it mixes with cool recharge waters from the surface. H_2S is oxidized to SO_4 and the resultant acidic SO_4-rich condensate fluid percolates down vertical structures, appearing as deep acid inflows in wells such as Pal-2D and Pal-9D. In wells CN-2RD and CN-3RD, temperature drops from 250°C to 215°C and y values are already near zero, indicating condensate liquid.

The hot degassing reservoir fluid flows through the lower layers of the volcanics formation and outflows towards the W-NW. This is shown by the negative y values of Pal-1RD, CN-1 and CN-3D. Temperature reversals are observed for the outflow-lying wells, e.g. Pal-1RD and Pal-3RD. These wells encounter cool dilute recharge fluids as well as acidic condensate fluids.

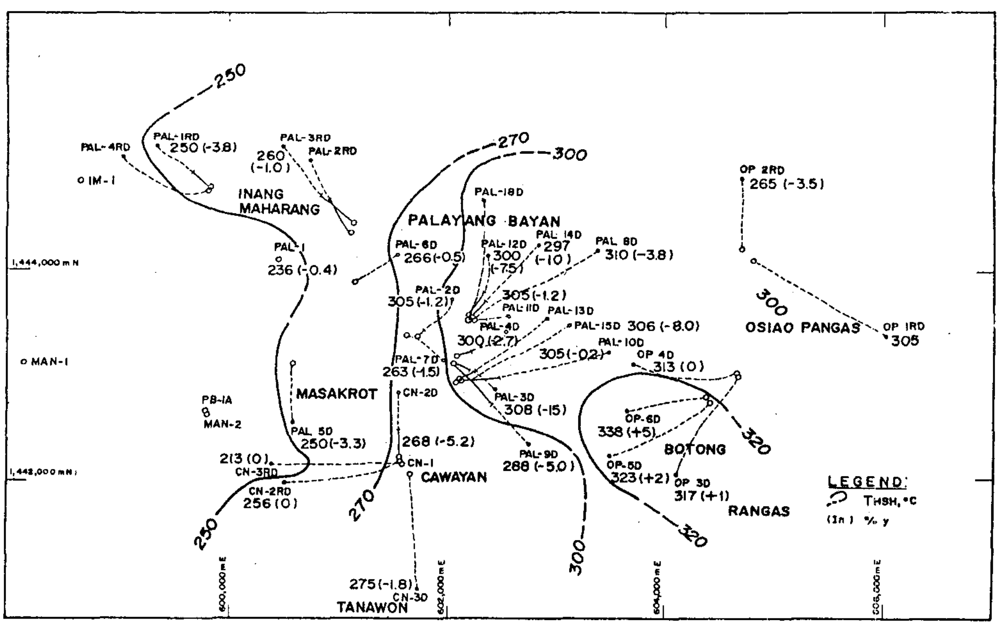

Fig. 5 Field Trends of THSH and Y

.5 0 .5 1 Km
GRAPHIC SCALE

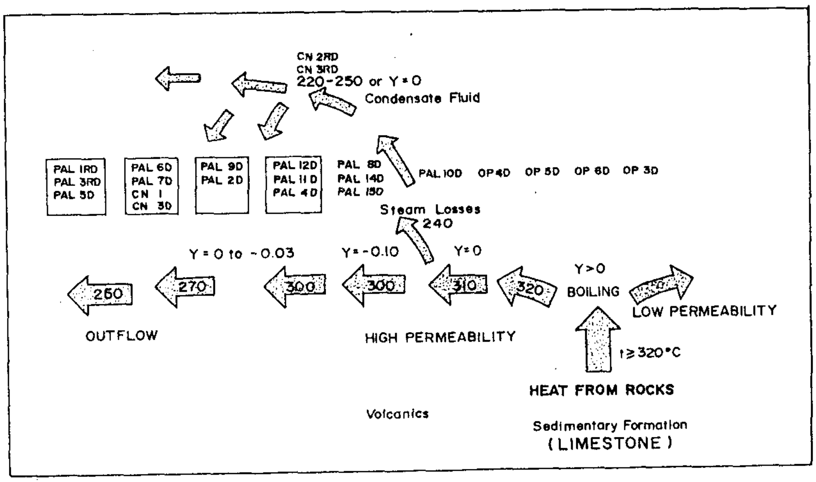

Fig. 6 Proposed BMGP Reservoir Model

CONCLUSIONS

The Fischer-Tropsch (FT) and H_2-H_2S (HSH) gas equilibria reactions are used in evaluating reservoir temperature and steam fraction. For BMGP wells with $y < -0.5\%$, the FT-HSH grid is not used and an approximate correction is made for H_2 that is lost due to preferential partitioning into the vapor phase and for the reequilibration of H_2S after steam loss.

Fair correlation is observed between T_{HSH}, quartz temperature (up to 300-320°C) and measured downhole temperatures in the majority of the wells. T_{HSH} is believed to give a good estimate of the local deep reservoir temperature. T_{HSH} is unaffected by acidic fluids, high discharge enthalpy (>1800 kj/kg), high CO_2 content in the reservoir fluid and despite also the fact that the major feed zone contributes a cooler dilute fluid.

A reservoir model is proposed. The primary reservoir fluid is slightly two-phase (y_{max}= 5%) and the main heat upflow zone is near the area delineated by the Botong wells, OP-3D to 6D. Permeability, as defined by vertical and horizontal structures, exerts control not only on the fluid outflow direction but also the gas composition. Deep reservoir boiling is caused by the shift from a less permeable sedimentary formation to more permeable volcanics. Gas composition is affected by postulated separate flow paths for a) the more mobile vapor phase which eventually forms a shallow condensate layer and, b) the deep hot degassed liquid.

ACKNOWLEDGEMENTS

The authors gratefully acknowledges the facilities, time and data provided by the management and staff of the Philippine National Oil Company- Energy Development Corporation (PNOC-EDC), the International Institute for Geothermal Research (CNR-IIRG) and International Atomic Energy Agency (IAEA).

REFERENCES

Aunzo, Z. P. 1990. GWELL: A Multi-Component Multi-Feedzone Geothermal Wellbore Simulator. M.Sc. Thesis, University of California, Berkeley, USA.

D'Amore, F., Nuti, S., Ruaya, J.R., Ramos-Candelaria, M.N., and Seastres, J.S. Jr., (in preparation) Applications of Gas Chemistry in Evaluating Physical Phenomena in Southern Negros (Palinpinon) Geothermal Field, Philippines.

D'Amore, F. and Truesdell, A.H. 1985. Calculation of geothermal reservoir temperatures and steam fractions from gas compositions. Geothermal Resources Council Transactions, v. 9.

Fournier, R.O. and Potter, R. W. 1982. A revised and expanded silica (quartz) geothermometer. Geotherm. Resource Council Bull., Nov. 1982, 3-12.

KRTA,Ltd., 1986. Bacon-Manito Geothermal Project: A Review of Gas Chemistry of Deep Wells, Internal Report.

PNOC-EDC, 1988. Bacman II Resource Assessment. PNOC Internal Report.